Title Page

Full head:

Manual and software-based measurements of treatment zone parameters and association of treatment zone parameters with axial elongation in orthokeratology

Running head: Treatment zone characteristics in orthokeratology

Keywords: treatment zone characteristics, orthokeratology, axial elongation, myopia control

Authors and affiliations:

Biyue Guo† BsC, Huihuan Wu‡ MsC, Sin Wan Cheung† PhD, and Pauline Cho† PhD

†Centre for Myopia Research, School of Optometry, The Hong Kong Polytechnic University, Kowloon, Hong Kong SAR, China

‡Department of Electrical Engineering, The Hong Kong Polytechnic University, Kowloon, Hong Kong SAR, China

Corresponding author:

Name: Biyue Guo; (+852)34002908

Email: ella.b.guo@polyu.edu.hk

Address: A136-137, Optometry Research Clinic, School of Optometry, The Hong Kong Polytechnic University, Hung Hum, Kowloon, Hong Kong SAR, China

Disclosure: None of the authors have a proprietary interest in any of the products mentioned.

Acknowledgements: The authors thank Dr Maureen Boost for her help with the editing of this manuscript. B. Guo is supported by the Research Residency Scheme of The Hong Kong Polytechnic University.

Abstract

Purpose: To compare the treatment zone (TZ) measurements obtained using manual and software-based methods in orthokeratology (ortho-k) subjects and explore the TZ characteristics of children with slow and fast axial elongation after ortho-k.

Methods: Data from 69 subjects (aged 7 – < 13 years old), who participated in three 24-month longitudinal orthokeratology studies, showing fast (> 0.27 mm, n = 38) and slow (< 0.09 mm, n = 31) axial elongation, were retrieved. The TZ after ortho-k was defined as central flattened area enclosed by points with no refractive power change. TZ parameters, including decentration, size, width of the peripheral steepened zone (PSZ), central and peripheral refractive power changes, and peripheral rate of power change, were determined manually and using a python-based software. TZ parameters were compared between measurement methods and between groups.

Results: Almost all TZ parameters measured manually and with the aid of a software were significantly different ($p < 0.05$). Differences in decentration, size, and the PSZ width were not clinically significant, but differences (0.45 to 0.92 D) in refractive power change in the PSZ were, although intraclass coefficients (0.945 to 0.978) indicated excellent agreement between methods. Significantly greater TZ decentration, smaller TZ size, and greater inferior rate of power change (relative to the TZ centre) were observed in slow progressors using both methods, suggesting a potential role of TZ in regulating myopia progression in ortho-k.

Conclusion: TZ measurements using manual and software-based methods differed significantly and cannot be used interchangeably. The combination of TZ decentration, TZ size, and peripheral rate of power change may affect myopia control effect in ortho-k.

Key points

- Treatment zone quantified manually and with the aid of a software were significantly different, but the differences may be clinically acceptable.
- Treatment zone decentration, TZ size, and inferior rate of power change (relative to the TZ centre) differ significantly between children with fast and slow axial elongation after orthokeratology treatment.
- Evaluation of treatment zone characteristics is valuable in orthokeratology and further studies are warranted to confirm its role in myopia control.

Introduction

The prevalence of myopia is higher in Chinese populations,[1,2] and continues to rise both here and elsewhere. Because of this upward trend[3,4] and its impact on ocular heath,[5] myopia has become a serious social and health concern worldwide. Researchers have developed various optical[6,7] and pharmaceutical methods[8-10] that can effectively retard myopia progression in school-aged children, of which atropine[9,10] and orthokeratology (ortho-k)[6,11] are currently most commonly prescribed by clinicians in East Asian countries.

Although its mechanism is not fully understood, ortho-k can slow axial elongation by 30 – 56% in children with low to moderate myopia and 63% in partially corrected high myopic children.[12] It has been hypothesized that altered relative periphery refraction[13,14] and higher order aberrations[15,16] are major contributing factors to its success in myopia control. Ortho-k treatment causes central corneal flattening and mid-peripheral corneal steepening. The central flattened area has been defined as the treatment zone (TZ) and the mid-peripheral steepened ring as the peripheral steepened zone (PSZ) in previous studies.[17,18] The PSZ was considered as part of the TZ in a previous study,[19] based on the assumption that the overall change in corneal shape[20] after ortho-k alters the higher order aberrations[19] and affects the visual quality,[21] which may retard myopia progression in children. However, few studies[19,20,22,23] have investigated the TZ and its correlation with peripheral refraction, higher order aberrations, and myopia progression.

Topographers, based on different measuring principles,[24] have been used in ortho-k to monitor changes to the corneal shape. Different topographical maps have been used to determine the TZ, including tangential,[19,22,23,25,26] axial,[18,27] and refractive[28,29] subtractive maps. Tangential maps measure the true corneal curvature, while axial maps measure the

radius of curvature with respect to the optical axis.[30] Refractive maps calculate true corneal refractive power, using Snell's law, and have been suggested to be the most accurate map for determining the TZ size,[31] although this has not been confirmed by a published study.[30] Whilst having limited accuracy to determine refractive power change, tangential subtractive maps provide sophisticated measurements of localized corneal changes and a better representation of the corneal shape after ortho-k,[31] and thus, were used to evaluate TZ characteristics in the current study.

Recent studies have reported an association between smaller TZ[22,23] and greater corneal peripheral power change[20] with slower axial elongation and a weak negative correlation between the TZ decentration and axial elongation.[26] Other TZ characteristics including, but not limited to, the PSZ width and peripheral rate of power change may also contribute to myopia control. However, previous studies investigating TZ parameters after ortho-k varied in methodologies, and the effect of TZ parameters on myopia progression remains unclear. Researchers have utilized several manual[20,22,23,25,26] and/or software-based[27,28] methods to determine TZ parameters, including the TZ size, the TZ central corneal power change, the PSZ width, peripheral power change, and the TZ decentration. Compared to manual methods, software-based methods allow more objective measurements and may be more efficient when used to investigate complicated research problems. However, to our knowledge, there is no reported paper comparing the agreement between manual and software-based measurements. This study aimed to compare the TZ parameters measured manually and with software and to explore TZ characteristics of children with slow and fast axial elongation after two years of ortho-k treatment.

Method

Study design

Data were retrieved from three 24-month longitudinal ortho-k studies (ROMIO,[11] TO-SEE,[32] and OKIC[33] studies) based on axial elongation of subjects after two years: fast progressors with axial elongation > 0.54 mm; slow progressors with axial elongation < 0.18 mm. All three studies were conducted according to the tenets of the Declaration of Helsinki, with ethics approved by the Human Subject Ethics Subcommittee of the School of Optometry of The Hong Kong Polytechnic University and written informed consent obtained from both subjects and parents. All studies were registered at ClinicalTrial.gov (ROMIO: NCT00962208, TO-SEE: NCT00978692, OKIC: NCT02643342). TZ parameters determined using measurement methods (manual vs software-based) and from different groups (fast progressors vs slow progressors) were compared.

Subjects

Subjects from the three studies (ROMIO,[11] TO-SEE,[32] and OKIC[33] studies) were aged 6 to < 13 years old with myopia no more than 5.00 D and astigmatism up to 3.50 D. They wore ortho-k lenses (Menicon Z Night or Z Night Toric, NKL Contactlenzen B.V.) in both eyes nightly during the 24-month longitudinal study period. Subjects from ROMIO[11] and TO-SEE[32] studies were fully corrected with ortho-k lenses, whereas the target correction remained unchanged from baseline for OKIC[33] subjects, with any residual refraction corrected using single-vision spectacles for daily wear.

At baseline and the 24-month visit, corneal topography (Medmont E300 Topographer, Medmont International Pty. Ltd., Nunawading, VIC, Australia) was performed before cycloplegia. Four topographical maps with similar shape were captured, with a maximum

difference of 0.25 D in central flat/steep K. Unaided and best-corrected visual acuity were measured by the Early Treatment Diabetic Retinopathy Study charts (Series 2000; Precision Vision, IL, USA) before cycloplegia. Cycloplegia was achieved by instillation of one drop of 0.5% proparacaine, 1% tropicamide, and 1% cyclopentolate five minutes apart in ROMIO[11] and TO-SEE[32] subjects. Two drops of 1% cyclopentolate were instilled in OKIC[33] subjects. Cycloplegic subjective refraction was determined using trial lenses according to the "maximum plus maximum visual acuity" rule. Axial length (IOLMaster 500; Carl Zeiss Meditec AG, Jena, Germany) was calculated as the average of five measurements with a maximum variance of 0.2 mm and ≥ 4 signal-to-noise ratios.

Determination of TZ parameters

The best topographical maps, at both the baseline and the 24-month visits, were selected for those with central flat/steep K and horizontal and vertical sagittal heights at the 9 mm chord closest to the average values of the four maps. The central flat/steep K was given precedent. For each subject, both manual and software-based measurements were obtained from the same topographical maps. Tangential subtractive maps (difference map between pre- and post-ortho-k treatment), representing tangential subtractive changes before and after ortho-k treatment, were used to determine TZ. TZ was defined as the central flattened area enclosed by points with zero refractive power change after ortho-k. TZ parameters were determined along the horizontal and vertical axes with respect to the TZ center (point O in Figure 1).

Manual measurement

Manual measurements of TZ were conducted by the same examiner involved in a previous study,[22] trained with sample topographical maps prior to performing the measurements and masked from the subjects' group during the measurements. TZ was determined following the

methodology described by Guo et al.[22] with a tolerance of ± 0.10 D for each zero point at the edge of the TZ. Briefly, the refractive power change was obtained by hovering the cursor above each reference point and the measurement shown on the image was recorded. Line segments AB and CD, shown in Figure 1, are the horizontal and vertical TZ diameters (the TZ size), respectively, which intercept at point O. TZ central dioptric power change was the refractive power change at this centre point, but it may not be the point with the greatest power change within the TZ. When hovering the cursor above the TZ centre, the distance (D) and angle (θ) from map centre to the TZ centre was shown below the color map (0.53 mm and 231º for point O in Figure 1), which was defined as the TZ decentration (vector form). TZ decentration along horizontal (x) and vertical (y) axes were calculated as shown: $x = D\cos\theta$, $y = D\sin\theta$, with positive signs representing nasal or superior decentration.

The TZ size was determined along the horizontal and vertical axes (Figure 1), with the distances between two reference points determined by the ruler function incorporated in the Medmont software, making the power change as close to zero as possible at each point. The PSZ was delineated as shown in Figure 1, with a peak rising from the edge of the TZ and returning to zero on the tangential subtractive map. The peak within the PSZ was determined as either the highest point with greatest power change or the turning point where the plateau was just reached (Figure 2A). A peak was considered missing if no plateau/highest point was definable within the PSZ (Figure 2B). The PSZ width was the distance between the two zero points on each side of the peak (temporal/nasal PSZ width: distances from AG/BH in Figure 1). A measurement was considered missing if no zero point could be determined on either side of the peak (Figure 2).

Induced peripheral myopic defocus was determined as the refractive power difference

between the highest peak and the TZ centre (temporal/nasal myopia defocus: power differences between points EO/FO in Figure 1). Peripheral rate of power change was determined as the slope of the lines AB, AC, and AO in Figure 3, connecting the PSZ peak (point A) to the zero point at TZ edge (point B), the point with greatest power change (point C), and the TZ centre (point O), respectively. The slope of the power change was estimated using the print-outs of the graphs. A scale of ± 15.00 D was applied for all subjects when screen-capturing the Medmont graphs. The distances between the reference points (eg. AB' and BB' in Figure 4) were obtained using the ruler tool in Adobe Photoshop 2020 (Adobe Inc., California, US). The distances obtained were then converted into refractive power differences (based on the scale and dimensions of the printouts) and horizontal/vertical displacements between the two reference points (eg. distance of line segment BB') to calculate the peripheral rates of power change (D/mm) along four directions (nasal, temporal, inferior, and superior).

Software-based measurement

Raw topographical data (tangential curvatures) from the baseline and 24-month visits were exported from Medmont topographer as mxf files. Each data file consisted of 50*50 points over a 12*12 mm^2 area, with adjacent points separated by 0.24 mm. Tangential curvatures at each point before and after ortho-k treatment were imported into a python-based (https://www.python.org/) software for analysis (Figure 4 (derived from the same subject and the same topographical maps pre- and post- ortho-k treatment as Figure 1)), with the following calculation: $Pt = \frac{336.5}{Rt}$, where Pt was the tangential power and Rt was the tangential curvature at each point. Additional data points were interpolated using a surface-fitting algorithm.[34] No filtering or error correcting algorithm was applied, resulting in minor

differences compared to the data presentation in Medmont software: less smooth spline and abrupt change at the limbal area representing measurement error/artifact (Figure 5). Best-fit ellipses were determined based on the contour lines consisting of "zero points", applying a least-square ellipse fitting algorithm.[35] The ellipse, located centrally and with the minimum enclosed area, was selected as the best-fit ellipse of TZ. The geometric centre of this best-fit ellipse was defined as the TZ centre and measurements were obtained along the horizontal and vertical axes of this ellipse. The x, y, and z coordinates of each reference point are illustrated in Figure 4, where x and y represent the distances to map centre (positive for nasal and superior directions) and z represents the refractive power change after ortho-k. TZ decentration was defined as the distance from geometric centre (0, 0) of map to the TZ centre (in vector form, with angle and total displacement). The amount of lens decentration along horizontal and vertical axes were also determined, with positive signs for nasal or superior decentration. TZ decentrations (x, y coordinates of TZ centre, and distance to TZ centre) and the TZ central dioptric power change (z coordinate of TZ centre) are presented below the color map. Other TZ parameters were calculated based on the coordinates of each reference point shown in Figure 4. For the PSZ peak and width measurements, data was considered missing if an abrupt change was noted as shown in Figure 5B. The slope of changes peripherally was calculated as the refractive power difference between the two reference points divided by their distances along x or y axis, with a unit of D/mm.

Statistical analysis

All statistical analyses were performed using SPSS 26.0 (IBM Corporation, Amonk, NY, US). Only data from the right eye was used for analysis. Normality of the data was investigated with the Shapiro-Wilk test. Paired-t tests and Wilcoxon signed-rank tests were used to compare the measurements obtained manually and with software, for normally

distributed and non-normally distributed data, respectively. Intraclass correlation coefficient (ICC) was calculated using the SPSS reliability analysis (results for single measures using two-way random model with absolute agreement). Unpaired-t tests and Mann-Whitney tests were performed to investigate the differences between fast and slow progressors, for normally distributed and non-normally distributed data, respectively. Sex composition was compared between groups using the Chi-square test. Two-tailed models were used for each analysis with a significance level set at 0.05.

Results

Baseline characteristics of slow and fast progressors

The slow progression group included 31 subjects (six from ROMIO, 13 from TO-SEE, and 12 from OKIC studies) and the fast progression group, 38 subjects (eight from ROMIO, eight from TO-SEE, and 22 from OKIC studies). Baseline and 24-month data for the slow progression (n = 31) and fast progression (n = 38) groups are listed in Table 1 and Table 2, respectively. Slow progressors were relatively older ($p < 0.001$) with longer baseline axial length ($p = 0.001$), more astigmatism ($p = 0.007$), and more negative spherical equivalent refraction (SER) ($p = 0.017$). After 24 months, slow progressors showed less negative residual refraction and SER, more astigmatism (similar to that noted at baseline), and better unaided visual acuity (Table 2).

Comparison between manual and software-based treatment zone measurements

Three subjects showed a false central island, thus measurements on the TZ central dioptric power change and slope to the TZ centre and most negative point were missing. One subject had a valid temporal PSZ width using manual measurement, but data with software was missing due to the ± 0.10 D tolerance adopted in manual measurements. On average, there

were 12%, 4%, 30%, and 10% subjects with missing measurements of the PSZ width in the temporal, nasal, inferior, and superior regions, respectively; and 0%, 0%, 7%, and 1% subjects with missing PSZ peak in the temporal, nasal, inferior, and superior regions, respectively, using both measurement methods. This resulted in relatively smaller sample sizes for width (slow progression: n = 24; fast progression: n =24) and peak (slow progression: n = 29; fast progression: n = 35) of inferior PSZ. All subjects had valid measurements on horizontal and vertical TZ sizes. The TZ decentration, using either methods, was mostly (manual: n = 51; software-based: n= 47) towards temporal (manual: -0.36 ± 0.21 (SD) mm; software-based: -0.41 ± 0.19 (SD) mm) and inferior (manual: -0.18 ± 0.22 (SD) mm; software-based: -0.16 ± 0.22 (SD) mm) directions.

All TZ parameters determined manually and using the software were significantly different ($p < 0.05$), except for TZ decentrations (displacement and vertical) in the slow progression group and the TZ central dioptric power change in both groups. Table 3 presents a summary of results for slow and fast progression groups. Differences in the TZ decentration, the TZ size, and the PSZ width were not clinically significant (within ± 0.10 mm), being less than the displacement between each data point in Medmont's exported file. Clinically significant differences (> 0.25 D) were noted in refractive power changes obtained at the PSZ peak, with an average of 0.47 D, 0.84 D, 0.85 D, and 0.76 D for the peaks of temporal, nasal, inferior, and superior PSZ. The ICCs were good to excellent (0.832 to 0.992) for manual and software-based measurements for all TZ parameters, except for the superior slope of change to TZ edge in fast progressors, ICC being 0.714.

Treatment zone characteristics in slow and fast progressors

Slow progressors showed significantly ($p < 0.05$) more TZ decentration (displacement and horizontal) and smaller TZ size (horizontal and vertical) compared to fast progressors, which were observed using both manual and software-based methods (Table 4). Refractive power change at the PSZ peak, peripheral myopic defocus, and the slope of refractive power change were not significantly different between the slow and fast progression groups, except for a significantly greater inferior slope of change to the TZ centre in slow progressors, using either measurement method ($p < 0.05$).

Discussion

A number of studies[17,19,22,23,26,36,37] have investigated TZ after ortho-k treatment. While most studies used manual measurements, a few measured TZ with the aid of a self-developed software.[18,27-29] In addition, different topographers, different topographical maps, and different methods have been used by these studies when determining TZ parameters, making it difficult to compare between manual and software-based methods among studies.

Previous studies have used various methods to manually measure TZ parameters. A range of topographers have been employed, including EyeSys[36] (http://eyesys.com/), Atlas Mastervue[19] (https://www.zeiss.com/), Pentacam[17] (https://www.oculus.com/), and Keratron Onda[23] (https://www.optikon.it/). Of the studies using Medmont topographer to evaluate TZ manually,[26,37] different topographical maps were selected. Sridharan and Swarbrick[37] determined TZ size and apical corneal refractive power change based on axial subtractive maps, while Chen et al.[26] determined the TZ size and decentration (to pupil centre) using tangential subtractive maps. Similarly, various software-based methods were selected by previous researchers. Of the studies using Medmont topographer for software analysis,

different raw data and different methods to determine best-fit ellipses were used. Faria-Ribeiro et al.[18] exported the raw evaluation data and calculated the mean curvature of each point, as the average of flat K and steep K. They applied a segmentation algorithm in Matlab to automatically define the central and peripheral zones for further analysis. Maseedupally et al.[29] utilized a modified manual method with Matlab analysis on TZ decentration, in which the Cartesian and polar grid printed on a transparent sheet, were placed over the computer screen to manually record the edge of the TZ. The 18 edge points displaced 20° apart were then entered into the Matlab software to fit the best ellipse. They defined the TZ decentration as a vector from map centre to the geometric centre of this ellipse. Gifford et al.[28] developed a Matlab software using raw sagittal heights to calculate the refractive power map and re-centred the map with respect to the centre of the entrance pupil. The software fitted the best ellipse based on the 12 "zero points" visually selected on this re-generated refractive map, separated by 30°. The authors defined TZ decentration as the distance from the entrance pupil to the centre of this ellipse. Hu et al.[27] used exported data on radial distances and axial curvatures, and re-generated the axial power map using an R program. They calculated the total corneal power shift along different concentric rings within the central 4 mm zone, and found this summed power shift negatively associated with axial elongation at 12 months.

Several studies have previously investigated TZ parameters using various methods, but none have compared TZ measurements obtained manually and using a software. The results of the current study show that TZ measurements determined in both ways showed poor agreement. In addition, previous studies have not reported use of regenerated Medmont's exported data (tangential subtractive maps) and fit best-fit ellipses directly from raw corneal curvatures. The current study is the first to present results in this way and to compare the refractive power differences obtained manually and with a software. As there are limited studies in this

area and the unknown algorithm applied in Medmont software, it is unclear which method (manual or software-based) is more accurate in measuring TZ parameters. Manual measurements are subjective and time consuming, but is a straightforward choice for researchers and practitioners without access to a software. The use of software, on the other hand, allows faster and more objective measurements, and can be used by less experienced examiners. Software is useful for research purposes as TZ parameters, other than the TZ size, can be easily measured and analysed. However, as the results of the current study indicated that only five TZ parameters (mostly TZ size and decentration) were significantly different between fast and slow progressors in ortho-k, the development of a specific software for TZ analysis may not be necessary.

The differences observed in the TZ decentration may be expected because the software utilized an ellipse fitting algorithm to obtain the centre of the TZ while the centre was approximately determined by the examiner using the manual method. Although the differences were minor, they may in turn cause differences in other TZ measurements. However, the between-method differences were less than the displacement of adjacent data points (0.24 mm), and the between-group differences using both methods were larger than this between-method difference. Hence, the observed differences in the TZ decentration may be negligible or clinically insignificant. It is possible that angle kappa could affect the measurements of lens decentration, however, as the data in this study is retrospective and the initial studies from which it emanated did not include this parameter, it was not possible to include angle kappa in the analysis. In addition, interaction between pupil size and the TZ size can affect the outcome of myopia control therapy. Therefore, measurements of both the pupil size and angle kappa will be considered in a future study.

Clinically significant differences in refractive power measurement (> 0.25 D) were noted between methods, with an average of 0.73 D, when determining the peak of the PSZ in different directions. This difference was also noted in the graphs presented by Medmont software and the software developed in this study, where the splines in the software were less smooth and showed abrupt changes in values, especially at the edge of the print-outs (> 9 mm chord) (Figure 5). The Medmont software conducted additional calculations for a particular point based on the values of the surrounding points, which filtered out the noise and errors when initially acquiring the tangential curvatures. In addition, the Medmont software may have applied a different interpolation algorithm compared to the current study. This resulted in a more regular and smoother spline compared to the raw data, but the algorithm for these calculations is a proprietary secret (personal communications with Medmont). However, despite the significant differences noted, the ICCs were good to excellent (> 0.830) for almost all TZ measurements, which suggest that the ICC should be used and interpreted with caution.[38]

Both methods revealed significantly greater TZ decentration, smaller TZ size, and greater inferior rate of power change (to the TZ centre) in slow progressors after ortho-k. Zhong et al.[20], reported a significant negative association between axial elongation over 24 months and temporal, nasal, and inferior maximum power change. In contrast, the current study showed that maximum refractive power changes (PSZ peaks) in all directions were not significantly different between fast and slow progressors. This may be due to different methods used: Zhong et al.[20] used TMS-4 topographer (TOMEY, Japan) to manually measure the sagittal power, whilst the current study used Medmont; Zhong et al.[20] used the 3-month topographical data to represent the post-ortho-k corneal changes, whereas the current study used 24-month topographical maps.

Results of the current study suggested that the TZ decentration, TZ size, and inferior rate of power change (relative to the TZ centre) were different between fast and slow progressors and may therefore play a role in effecting myopia control using ortho-k lenses. However, because of significant differences in baseline characteristics (e.g. age, axial length, and SER) between fast and slow progressors, the effect of TZ on axial elongation warrants further investigation.

Conclusion

In conclusion, TZ measurements obtained using manual and software-based methods were significantly different, but the differences in the TZ decentration, TZ size, and PSZ width were clinically acceptable. Differences in measurements of refractive power change were clinically significant between methods, but this was likely to be due to the additional filtering and error-correcting algorithm incorporated in the Medmont topographer. TZ characteristics may play a role in myopia control in ortho-k, but further confirmatory studies are warranted.

Table 1. Demographics and baseline data of orthokeratology subjects with slow (SP) and fast (FP) progression (Mean ± SD or Median [Min, Max])

	SP group (n = 31)	**FP group (n = 38)**	**P**
Age (years)	9.85 ± 1.23	8.61 ± 0.94	< 0.001*
Male/Female	16/15	14/24	0.218
Axial length (mm)	24.74 ± 0.76	24.14 ± 0.74	0.001*
Spherical refraction (D)	-2.49 ± 1.10	-2.06 ± 0.96	0.085
Refractive astigmatism (D)	-1.00 [-2.75, 0.00]	-0.50 [-2.50, 0.00]	0.007*
SER (D)	-3.04 ± 1.26	-2.36 ± 1.04	0.017*
BCVA (logMAR)	-0.02 ± 0.06	-0.01 ± 0.07	0.781

* Significant difference between slow and fast progression groups.

SER – spherical equivalent refractive error; BCVA – best-corrected visual acuity; P – probability value of unpaired-t or Mann-Whitney U tests for differences between groups

Table 2. Residual cycloplegic subjective refraction and visual acuity measurements of orthokeratology subjects with slow (SP) and fast (FP) progression at the 24-month visit (Mean ± SD or Median [Min, Max])

	SP group (n = 31)	**FP group (n = 38)**	**P**
Axial elongation (mm)	0.06 [-0.29, 0.17]	0.68 [0.55, 1.35]	< 0.001*
Spherical refraction (D)	0.50 [-0.50, 1.50]	-0.25 [-2.25, 0.50]	< 0.001*
Refractive astigmatism (D)	-0.75 [-1.50, 0.00]	-0.50 [-1.75, 0.00]	0.018*
SER (D)	0.00 [-1.00, 0.88]	-0.44 [-2.63, 0.50]	< 0.001*
BCVA (logMAR)	-0.04 ± 0.06	-0.04 ± 0.06	0.827
UVA (logMAR)	0.00 [-0.14, 0.14]	0.06 [-0.16, 0.92]	0.020*

* Significant difference between groups.

SER – spherical equivalent refraction; BCVA – best-corrected visual acuity; UVA – uncorrected visual acuity; P – probability value of unpaired-t or Mann-Whitney U tests for differences between groups

Table 3. Comparison of treatment zone (TZ) measurements determined by the manual and the software-based methods (Mean ± SD or Median [Min, Max]) in slow (SP) and fast (FP) progressors

TZ parameters	SP group					FP group				
	Manual	Software-based	ICC	P	Mean differences ± SD	Manual	Software-based	ICC	P	Mean differences ± SD
Displacement of decentration (mm)	0.54 ± 0.22	0.55 ± 0.21	0.964	0.28	0.01 ± 0.06	0.40 ± 0.17	0.45 ± 0.17	0.928	< 0.001	0.05 ± 0.04
Decentration (x, positive for nasal) (mm)	-0.44 ± 0.24	-0.47 ± 0.22	0.970	0.01	-0.03 ± 0.05	-0.29 ± 0.15	-0.37 ± 0.15	0.859	< 0.001	-0.08 ± 0.04
Decentration (y, positive for superior) (mm)	-0.20 ± 0.20	-0.18 ± 0.22	0.910	0.14	0.02 ± 0.09	-0.16 ± 0.23	-0.14 ± 0.22	0.964	0.01	0.02 ± 0.06
TZ center dioptric change (D)	-2.74 ± 0.94	-2.76 ± 0.92	0.995	0.274	-0.02 ± 0.09	-2.62 ± 0.89	-2.64 ± 0.89	0.994	0.238	-0.02 ± 0.10
Horizontal TZ size (mm)	3.07 ± 0.49	3.13 ± 0.49	0.989	< 0.001	0.06 ± 0.04	3.64 ± 0.60	3.70 ± 0.60	0.992	< 0.001	0.07 ± 0.04
Vertical TZ size (mm)	3.18 ± 0.47	3.28 ± 0.44	0.916	0.002	0.10 ± 0.16	3.47 ± 0.42	3.53 ± 0.43	0.986	< 0.001	0.06 ± 0.04
Temporal PSZ width (mm)	1.48 [0.81, 2.96]	1.44 [0.77, 2.97]	0.984	< 0.001	-0.03 ± 0.06	1.54 [1.13, 2.29]	1.51 [1.08, 2.00]	0.930	< 0.001	-0.06 ± 0.06
Nasal PSZ width (mm)	1.44 [0.98, 2.16]	1.42 [0.92, 2.18]	0.982	< 0.001	-0.03 ± 0.04	1.45 [1.05, 2.91]	1.42 [1.01, 2.83]	0.986	< 0.001	-0.04 ± 0.02
Inferior PSZ width (mm)	1.44 [0.87, 2.39]	1.41 [0.87, 2.36]	0.988	< 0.001	-0.05 ± 0.03	1.50 ± 0.30	1.46 ± 0.31	0.984	< 0.001	-0.04 ± 0.04
Superior PSZ width (mm)	1.46 ± 0.24	1.43 ± 0.24	0.985	< 0.001	-0.03 ± 0.02	1.48 [1.09, 2.74]	1.42 [-1.40, 2.54]	0.832	< 0.001	-0.09 ± 0.17
Temporal peak power (D)	4.59 ± 2.39	5.04 ± 2.63	0.978	< 0.001	0.45 ± 0.29	4.66 [1.74, 13.67]	5.07 [1.77, 15.88]	0.975	< 0.001	0.49 ± 0.38
Nasal peak power (D)	6.61 ± 3.08	7.47 ± 3.60	0.954	< 0.001	0.86 ± 0.58	6.16 [2.40, 13.69]	6.93 [2.68, 15.81]	0.961	< 0.001	0.81 ± 0.44
Inferior peak power (D)	7.90 ± 3.13	8.82 ± 3.59	0.949	< 0.001	0.92 ± 0.61	6.70 ± 3.20	7.47 ± 3.65	0.962	< 0.001	0.78 ± 0.56
Superior peak power (D)	6.78 ± 2.77	7.56 ± 3.14	0.953	< 0.001	0.78 ± 0.50	6.74 ± 2.28	7.48 ± 2.50	0.945	< 0.001	0.74 ± 0.33
Temporal defocus (D)	7.15 ± 3.26	7.62 ± 3.46	0.987	< 0.001	0.47 ± 0.27	7.31 [3.53, 17.04]	7.76 [3.66, 19.51]	0.981	< 0.001	0.51 ± 0.41
Nasal defocus (D)	9.17 ± 3.83	10.05 ± 4.28	0.968	< 0.001	0.88 ± 0.55	8.46 [4.09, 17.54]	9.17 [4.45, 19.57]	0.971	< 0.001	0.83 ± 0.43
Inferior defocus (D)	10.53 ± 3.92	11.46 ± 4.37	0.967	< 0.001	0.93 ± 0.57	9.22 ± 3.81	10.00 ± 4.21	0.973	< 0.001	0.78 ± 0.54
Superior defocus (D)	9.39 ± 3.67	10.18 ± 4.03	0.971	< 0.001	0.79 ± 0.50	9.29 ± 2.73	10.05 ± 2.92	0.959	< 0.001	0.76 ± 0.33
Temporal slope (to TZ edge) (D/mm)	5.47 ± 2.62	6.64 ± 3.36	0.879	< 0.001	1.17 ± 1.01	5.93 ± 2.74	6.77 ± 2.99	0.927	< 0.001	0.84 ± 0.76
Temporal slope (to TZ center) (D/mm)	3.07 ± 1.20	3.39 ± 1.38	0.952	< 0.001	0.32 ± 0.26	2.83 [1.01, 5.75]	3.10 [1.21, 6.20]	0.964	< 0.001	0.27 ± 0.21
Temporal slope (to the point with most negative power change) (D/mm)	3.51 ± 1.46	3.99 ± 1.57	0.867	0.001	0.48 ± 0.66	3.33 ± 1.42	3.60 ± 1.56	0.925	0.004	0.27 ± 0.52
Nasal slope (to TZ edge) (D/mm)	7.38 [1.74, 19.92]	9.16 [1.79, 28.61]	0.837	< 0.001	1.96 ± 2.46	7.53 ± 3.34	9.08 ± 4.07	0.878	< 0.001	1.55 ± 1.14
Nasal slope (to TZ center) (D/mm)	4.03 ± 1.84	4.35 ± 2.05	0.969	< 0.001	0.32 ± 0.37	3.07 [1.47, 6.98]	3.40 [1.57, 7.37]	0.973	< 0.001	0.27 ± 0.23
Nasal slope (to the point with most negative power change) (D/mm)	3.94 ± 1.90	4.32 ± 2.16	0.962	< 0.001	0.38 ± 0.42	3.06 [1.25, 8.93]	3.43 [1.53, 11.07]	0.896	< 0.001	0.58 ± 0.88

Inferior slope (to TZ edge) (D/mm)	9.37 ± 4.30	11.38 ± 5.64	0.869	< 0.001	2.00 ± 1.78	6.43 [2.05, 22.61]	8.38 [2.18, 27.95]	0.871	< 0.001	1.85 ± 2.03
Inferior slope (to TZ center) (D/mm)	4.61 ± 1.70	5.07 ± 1.97	0.947	< 0.001	0.46 ± 0.41	3.03 [1.33, 8.70]	3.44 [1.39, 9.50]	0.973	< 0.001	0.30 ± 0.34
Inferior slope (to deepest point) (D/mm)	4.08 [2.11, 12.29]	4.61 [2.16, 18.29]	0.905	<0.001	1.10 ± 1.40	3.65 [1.39, 12.03]	4.26 [1.42, 14.82]	0.907	< 0.001	0.94 ± 1.00
Superior slope (to TZ edge) (D/mm)	8.17 ± 3.39	9.67 ± 4.57	0.859	< 0.001	1.50 ± 1.64	7.77 ± 2.59	9.08 ± 3.19	0.714	< 0.001	1.31 ± 1.91
Superior slope (to TZ center) (D/mm)	3.91 ± 1.55	4.33 ± 1.80	0.949	< 0.001	0.42 ± 0.35	3.50 ± 1.06	3.82 ± 1.13	0.944	< 0.001	0.32 ± 0.20
Superior slope (to the point with greatest power change) (D/mm)	4.34 ± 2.01	4.74 ± 2.33	0.956	0.001	0.39 ± 0.53	3.74 [1.48, 5.75]	3.85 [1.64, 8.45]	0.862	0.002	0.17 ± 0.88

458 PSZ – peripheral steepened zone; ICC – intraclass correlation coefficient; P – probability value of paired-*t* or Wilcoxon signed-rank tests for differences between manual and software-based
459 measurement

460

461

Table 4. Comparison of treatment zone (TZ) parameters between slow (SP) and fast (FP) progressors using manual and software-based methods (Mean ± SD or Median [Min, Max])

TZ parameters†	Manual			Software-based		
	SP group	FP group	P	SP group	FP group	P
Displacement of decentration (mm)	0.54 ± 0.22	0.40 ± 0.17	0.005*	0.55 ± 0.21	0.45 ± 0.17	0.034*
Decentration (x, positive for nasal) (mm)	-0.44 ± 0.24	-0.29 ± 0.15	0.003*	-0.47 ± 0.22	-0.37 ± 0.15	0.034*
Horizontal TZ size (mm)	3.07 ± 0.49	3.64 ± 0.60	< 0.001*	3.13 ± 0.49	3.70 ± 0.60	< 0.001*
Vertical TZ size (mm)	3.18 ± 0.47	3.47 ± 0.42	0.008*	3.28 ± 0.44	3.53 ± 0.43	0.020*
Inferior slope (to TZ center) (D/mm)	4.35 [1.87, 8.58]	3.03 [1.33, 8.70]	0.027*	5.01 [2.01, 9.52]	3.44 [1.39, 9.50]	0.025*

* Significant difference between groups.

†Only parameters which were significantly different between groups are presented

P – probability value of unpaired-t or Mann-Whitney U tests for differences between groups

Figure 1. Illustration of treatment zone determination and referent points for treatment zone measurements using the manual method, (tangential subtractive map of Medmont derived from the same subject and the same topographical maps pre- and post-orthokeratology treatment as Figure 4). AB represents the treatment zone (TZ) and AG/BH, the temporal/nasal peripheral steepened zone (PSZ).

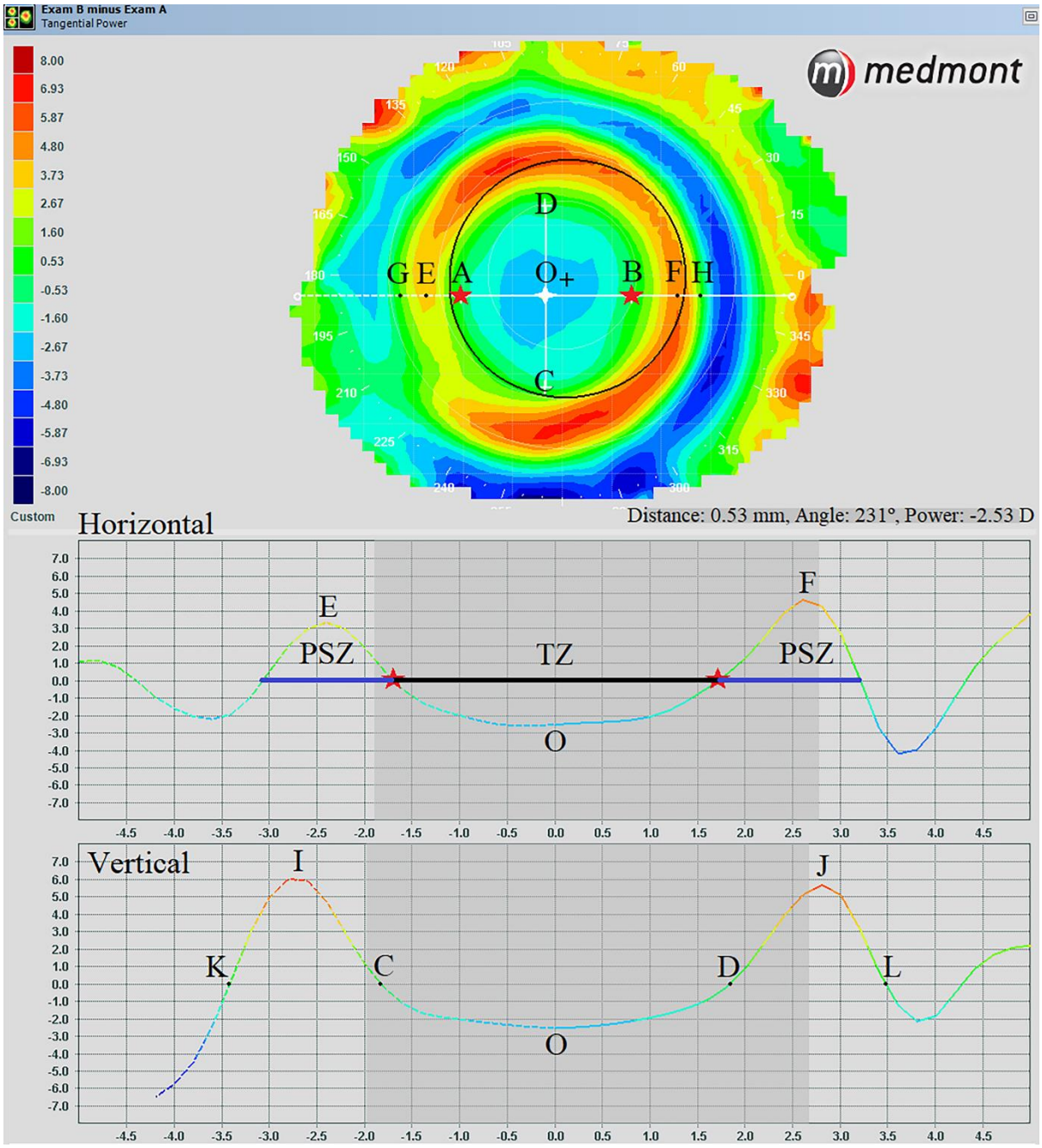

Figure 2. Illustration of definable and undefinable peripheral steepened zone (PSZ) peak and width under different conditions. A: Definable PSZ peak and width at point B; definable PSZ peak, but undefinable PSZ width at point A. B: Undefinable PSZ peak and width beyond point C.

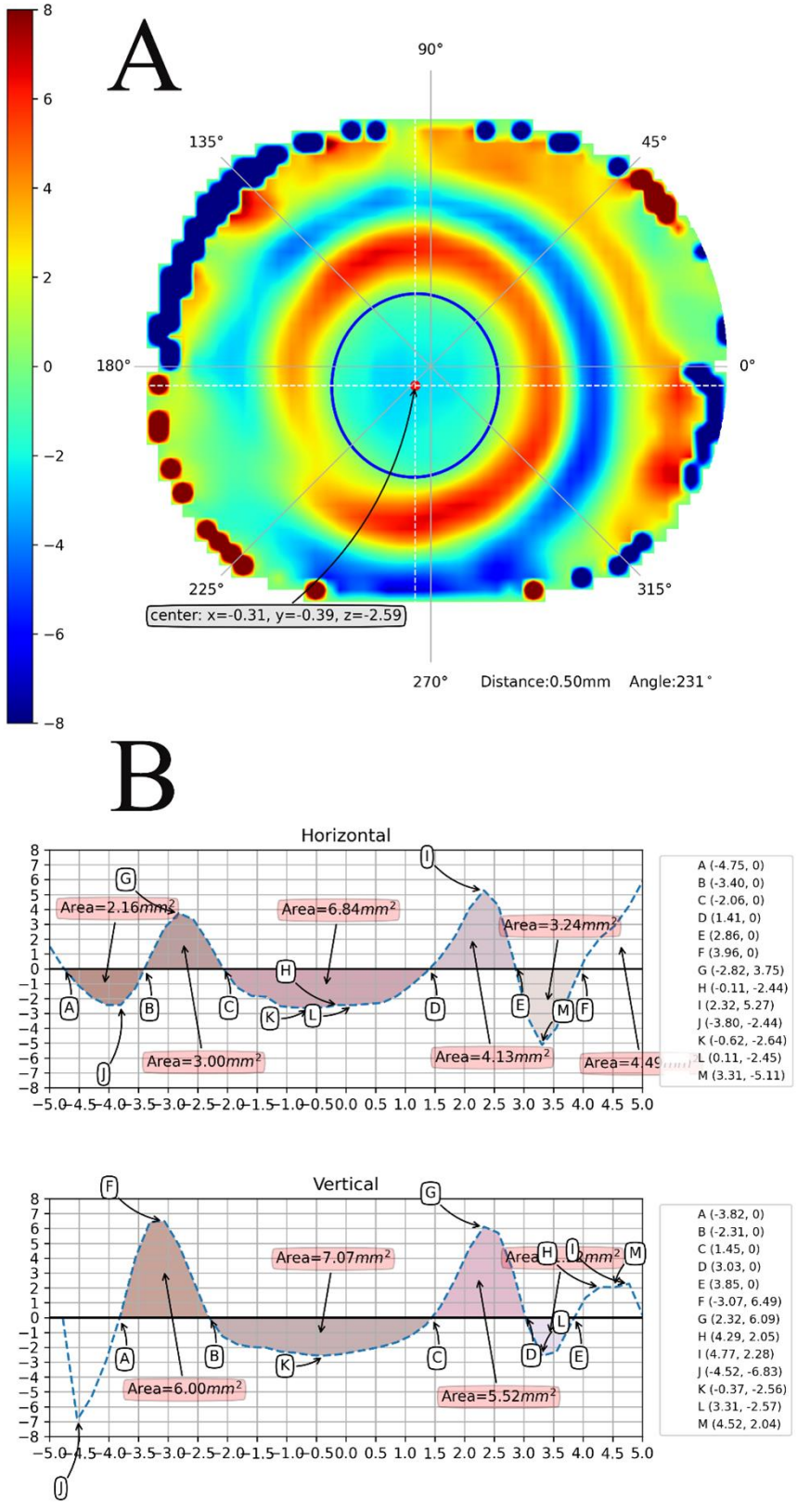

Figure 3. Determination of different rates of peripheral refractive power change. Line segments AB, AC, and AO represent the slopes of change from peripheral peak (point A) to the zero point at treatment zone edge (point B), point with most negative power change (point C), and treatment zone centre (point O), respectively.

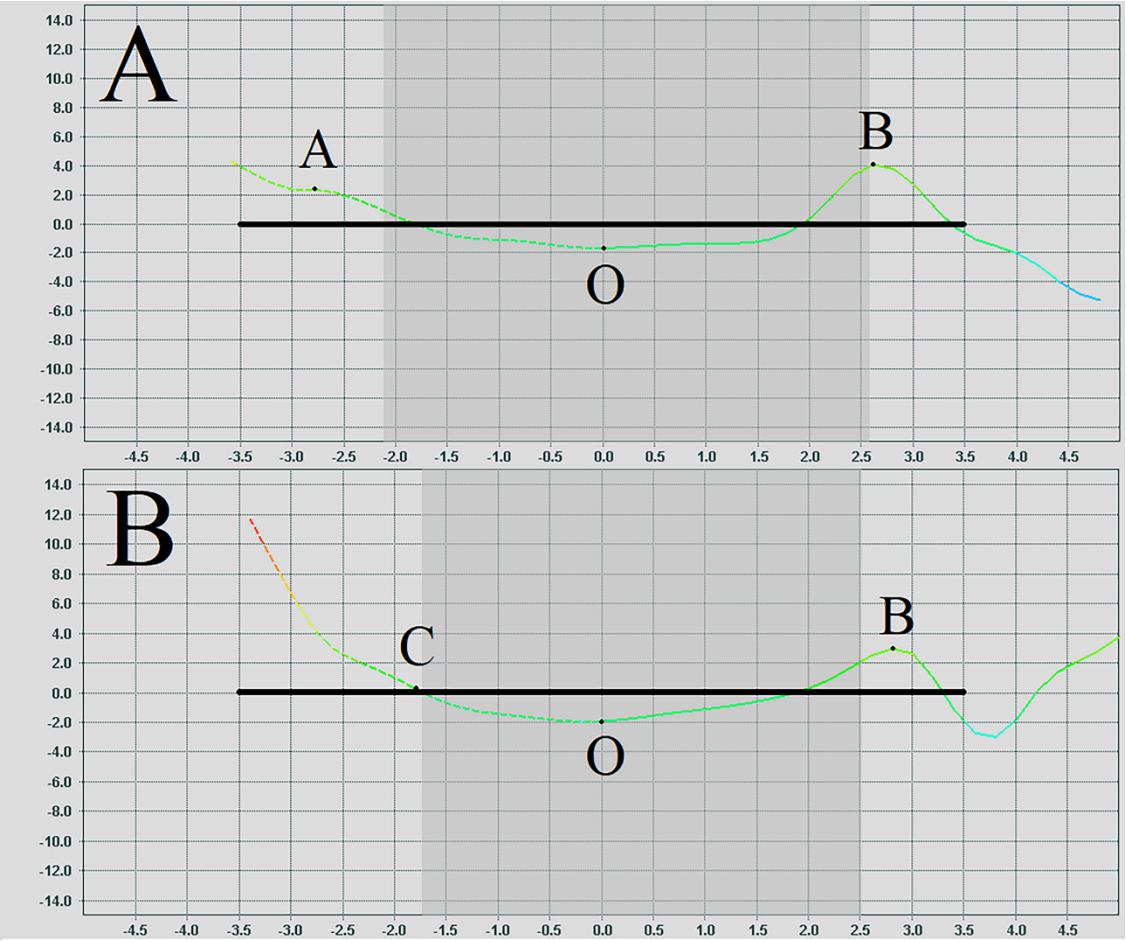

Figure 4. Illustration of treatment zone measurement using software-based method. A: Map generated by a python-based software, using tangential data (curvatures) exported from Medmont. B: Illustration of referent points for treatment zone measurements (derived from the same subject and the same topographical maps pre- and post-orthokeratology treatment as Figure 1).

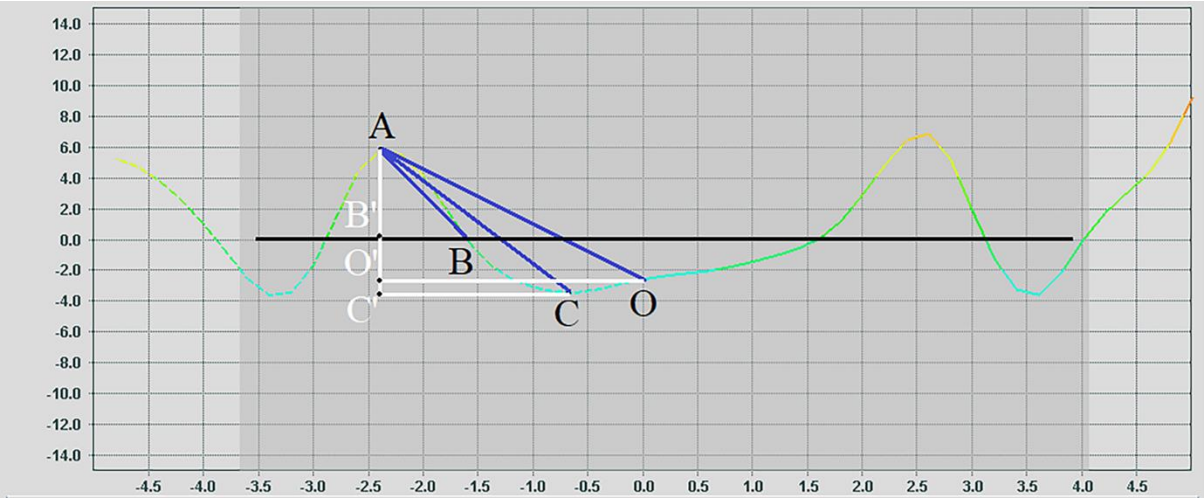

Figure 5. Illustration of differences in data presentation between the python-based software (A) and Medmont software (B). Refractive power changes are different between points E and E', and I and I'. An abrupt change is seen at point A in the python-based software, compared with point A' in the Medmont software.

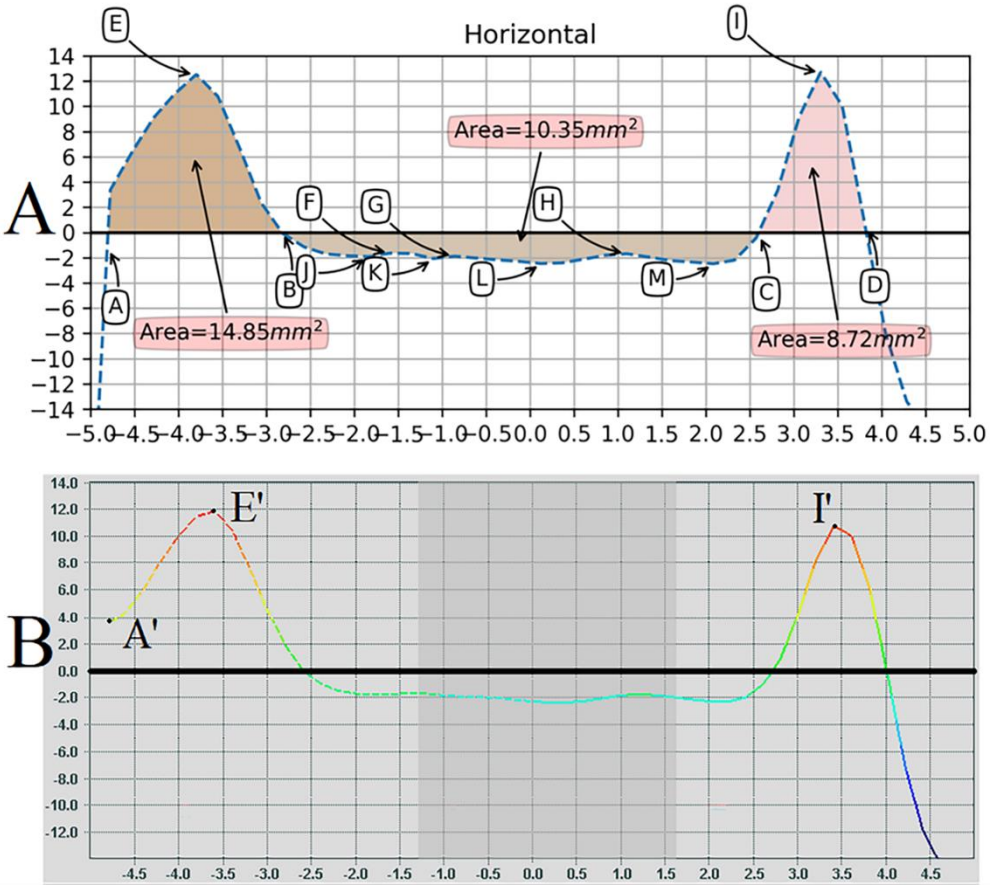

References

1. Zhou WJ, Zhang YY, Li H et al. Five-year progression of refractive errors and incidence of myopia in school-aged children in Western China. *J Epidemiol* 2016; 26: 386-395.
2. Lin L, Shih Y, Hsiao C & Chen C. Prevalence of myopia in Taiwanese schoolchildren: 1983 to 2000. *Ann Acad Med* 2004; 33: 27-33.
3. Vitale S, Sperduto RD & Ferris FL. Increased prevalence of myopia in the united states between 1971-1972 and 1999-2004. *Arch Ophthalmol* 2009; 127: 1632-1639.
4. Chen M, Wu A, Zhang L et al. The increasing prevalence of myopia and high myopia among high school students in Fenghua city, eastern China: a 15-year population-based survey. *BMC Ophthalmol* 2018; 18: 159.
5. Haarman AE, Enthoven CA, Tideman JWL, Tedja MS, Verhoeven VJ & Klaver CC. The complications of myopia: a review and meta-analysis. *Invest Ophthalmol Vis Sci* 2020; 61: 49.
6. Santodomingo-Rubido J, Villa-Collar C, Gilmartin B & Gutiérrez-Ortega R. Myopia control with orthokeratology contact lenses in Spain: refractive and biometric changes. *Invest Ophthalmol Vis Sci* 2012; 53: 5060-5065.
7. Walline JJ, Walker MK, Mutti DO et al. Effect of high add power, medium add power, or single-vision contact lenses on myopia progression in children: the BLINK randomized clinical trial. *JAMA Ophthalmol* 2020; 324: 571-580.
8. Siatkowski RM, Cotter SA, Crockett R et al. Two-year multicenter, randomized, double-masked, placebo-controlled, parallel safety and efficacy study of 2% pirenzepine ophthalmic gel in children with myopia. *J AAPOS* 2008; 12: 332-339.
9. Chua WH, Balakrishnan V, Chan YH et al. Atropine for the treatment of childhood myopia. *Ophthalmology* 2006; 113: 2285-2291.
10. Yam JC, Jiang Y, Tang SM et al. Low-concentration atropine for myopia progression (LAMP) study: A randomized, double-blinded, placebo-controlled trial of 0.05%, 0.025%, and 0.01% atropine eye drops in myopia control. *Ophthalmology* 2019; 126: 113-124.
11. Cho P & Cheung SW. Retardation of myopia in orthokeratology (ROMIO) study: a 2-year randomized clinical trial. *Invest Ophthalmol Vis Sci* 2012; 53: 7077-7085.
12. Vincent SJ, Cho P, Chan KY et al. CLEAR – orthokeratology. *Cont Lens Anterior Eye* 2021; 44: 240-269.
13. Kang P & Swarbrick H. Peripheral refraction in myopic children wearing orthokeratology and gas-permeable lenses. *Optom Vis Sci* 2011; 88: 476-482.
14. Charman WN, Mountford J, Atchison DA & Markwell EL. Peripheral refraction in orthokeratology patients. *Optom Vis Sci* 2006; 83: 641-648.
15. Lau JK, Vincent SJ, Cheung SW & Cho P. Higher-order aberrations and axial elongation in myopic children treated with orthokeratology. *Invest Ophthalmol Vis Sci* 2020; 61: 22.

16. Hiraoka T, Kakita T, Okamoto F & Oshika T. Influence of ocular wavefront aberrations on axial length elongation in myopic children treated with overnight orthokeratology. *Ophthalmology* 2015; 122: 93-100.
17. Carracedo G, Espinosa-Vidal T, Martínez-Alberquilla I & Batres L. The topographical effect of optical zone diameter in orthokeratology contact lenses in high myopes. *J Ophthalmol* 2019; doi: 10.1155/2019/1082472, accessed 11/12/2020.
18. Faria-Ribeiro M, Belsue RN, López-Gil N & González-Méijome JM. Morphology, topography, and optics of the orthokeratology cornea. *J Biomed Opt* 2016; 21: 075011.
19. Lu F, Simpson T, Sorbara L & Fonn D. The relationship between the treatment zone diameter and visual, optical, and subjective performance in Corneal Refractive Therapy lens wearers. *Ophthalmic Physiol Opt* 2007; 27: 568-578.
20. Zhong Y, Chen Z, Xue F, Zhou J, Niu L & Zhou X. Corneal power change is predictive of myopia progression in orthokeratology. *Optom Vis Sci* 2014; 91: 404-411.
21. Hiraoka T, Okamoto C, Ishii Y, Kakita T & Oshika T. Contrast sensitivity function and ocular higher-order aberrations following overnight orthokeratology. *Invest Ophthalmol Vis Sci* 2007; 48: 550-556.
22. Guo B, Cheung SW, Kojima R & Cho P. One-year results of the Variation of Orthokeratology Lens Treatment Zone (VOLTZ) Study: a prospective randomised clinical trial. *Ophthalmic Physiol Opt* 2021; 41: 702-714.
23. Pauné J, Fonts S, Rodríguez L & Queirós A. The role of back optic zone diameter in myopia control with orthokeratology lenses. *J Clin Med* 2021; 10: 336.
24. Wang Q, Savini G, Hoffer KJ et al. A comprehensive assessment of the precision and agreement of anterior corneal power measurements obtained using 8 different devices. *PloS One* 2012; 7: e45607.
25. Wang A & Yang C. Influence of overnight orthokeratology lens treatment zone decentration on myopia progression. *J Ophthalmol* 2019; doi: https://doi.org/10.1155/2019/2596953, accessed 24/6/2021.
26. Chen R, Chen Y, Lipson M et al. The effect of treatment zone decentration on myopic progression during or-thokeratology. *Curr Eye Res* 2020; 45: 645-651.
27. Hu Y, Wen C, Li Z, Zhao W, Ding X & Yang X. Areal summed corneal power shift is an important determinant for axial length elongation in myopic children treated with overnight orthokeratology. *Br J Ophthalmol* 2019; 103: 1571-1575.
28. Gifford P, Tran M, Priestley C, Maseedupally V & Kang P. Reducing treatment zone diameter in orthokeratology and its effect on peripheral ocular refraction. *Cont Lens Anterior Eye* 2020; 43: 54-59.

628 29. Maseedupally VK, Gifford P, Lum E et al. Treatment zone decentration during
629 orthokeratology on eyes with corneal toricity. *Optom Vis Sci* 2016; 93: 1101-1111.
630 30. Maseedupally VK. Regional corneal topographic responses in overnight orthokeratology and
631 their influence on treatment zone decentration [thesis]: The University of New South Wales Sydney,
632 Australia; 2013.
633 31. Mountford J. Corneal and refractive changes due to orthokeratology. In: Orthokeratology:
634 Principles and Practice (Benson K, editor), London: Butterworth-Heinemann Medical, 2004; pp. 175-
635 202.
636 32. Chen C, Cheung SW & Cho P. Myopia control using toric orthokeratology (TO-SEE study).
637 *Invest Ophthalmol Vis Sci* 2013; 54: 6510-6517.
638 33. Wan K, Lau JK, Cheung SW & Cho P. Orthokeratology with increased compression factor
639 (OKIC): study design and preliminary results. *BMJ Open Ophthalmol* 2020; 5: e000345.
640 34. Dierckx P. An algorithm for surface-fitting with spline functions. *IMA J Numer Anal* 1981; 1:
641 267-283.
642 35. Halır R & Flusser J, editors. Numerically stable direct least squares fitting of ellipses.
643 Proceedings of the Sixth International Conference on Computer Graphics and Visualization; 1998.
644 36. Tahhan N, Du Toit R, Papas E, Chung H, La Hood D & Holden. Comparison of reverse-
645 geometry lens designs for overnight orthokeratology. *Optom Vis Sci* 2003; 80: 796-804.
646 37. Sridharan R & Swarbrick H. Corneal response to short-term orthokeratology lens wear.
647 *Optom Vis Sci* 2003; 80: 200-206.
648 38. Guo B, Lau JK, Cheung SW & Cho P. Repeatability and reproducibility of manual choroidal
649 thickness measurement using Lenstar images in children before and after orthokeratology treatment
650 *Cont Lens Anterior Eye* 2021; doi: 10.1016/j.clae.2021.101484, accessed 3/9/2021.
651